IEEE Access
Multidisciplinary ⋮ Rapid Review ⋮ Open Access Journal

Received September 30, 2016, accepted October 19, 2016, date of publication January 16, 2017, date of current version March 2, 2017.

Digital Object Identifier 10.1109/ACCESS.2016.2644662

An EEMD Aided Comparison of Time Histories and Its Application in Vehicle Safety

ZUOLONG WEI[1], (Member, IEEE), KJELL GUNNAR ROBBERSMYR[1], (Senior Member, IEEE), AND HAMID REZA KARIMI[2], (Senior Member, IEEE)

[1]Department of Engineering, Faculty of Engineering and Science, University of Agder, 4879 Grimstad, Norway
[2]Department of Mechanical Engineering, Politecnico di Milano, 20156 Milan, Italy

Corresponding author: Z. Wei (zuolong.wei@uia.no)

ABSTRACT In the context of signal processing, the comparison of time histories is required for different purposes, especially for the model validation of vehicle safety. Most of the existing metrics focus on the mathematical value only. Therefore, they suffer the measuring errors, disturbance, and uncertainties and can hardly achieve a stable result with a clear physical interpretation. This paper proposes a novel scheme of time histories comparison to be used in vehicle safety analysis. More specifically, each signal for comparison is decomposed into a trend signal and several intrinsic mode functions (IMFs) by ensemble empirical mode decomposition. The trend signals reflect the general variation and are free from the influence of high-frequency disturbances. With the help of dynamic time warping, the errors of time and magnitude between trends are calculated. The IMFs, which contain high-frequency information, are compared on frequency, magnitude, and local features. To illustrate the full scope and effectiveness of the proposed scheme, this paper provides three vehicle crash cases.

INDEX TERMS Time-history, model validation, Ensemble Empirical Mode Decomposition (EEMD), dynamic time warping (DTW), vehicle crash.

I. INTRODUCTION

Time histories can present the variation of signals over time and are often used to record the detailed processes of events. In some areas, such as pattern recognition, fault diagnosis, data mining and numerical simulations, an objective, proper and accurate comparison is in great request [1]. An integrated scheme of comparison contains the pre-process, discrepancy calculation and optional post-process (e.g. the evaluation of discrepancies). Typically, the fundamental problem is to define a proper comparison metric, which refers to mathematical measures that quantify the level of agreement between different signals, for the discrepancy calculation [2]. According to the features of signals and the purposes of comparison, the metrics should be diverse in different applications.

One of the purposes of time histories comparison is to validate computational models, a critical topic of numerical simulation, which is particularly rigorous in the field of vehicle safety. More specifically, the validation process is to assess to which degree that the simulation can replicate the corresponding physical event [3]. In the context of vehicle safety, the crashes are usually recorded by electronic and photographic instruments [4], [5]. And model validation is normally conducted by quantitative comparisons of response signals, i.e. the accelerations during crashes and simulations, which are measured by accelerometers. Therefore, both engineering and academic researchers developed many comparison metrics to achieve an accurate and reliable validation for simulations of vehicle safety. However, as far as the authors' knowledge, these developed metrics focus on the mathematical value only and ignore the physical meaning of the comparative signals.

In this paper, the existing metrics are presented firstly with respect to their advantages and disadvantages. Then a signal processing methodology is proposed to be involved in the comparison process. More specifically, the signals are decomposed by the Ensemble Empirical Mode Decomposition (EEMD) algorithm in different frequency domains. This makes it possible to introduce more features into the detailed comparison, which will consequently improve the performance of comparisons. Although emphasizes on the application in vehicle safety, the proposed metric is universal and can be introduced into related fields.

The remainder of this paper is organized as follows. Section II reviews and analyses the existing metrics. A discussion about the comparison metrics is also given in this section. In Section III, the proposed comparison scheme and related technologies are presented in detail. The next section shows some case studies of the vehicle crashes to show the

TABLE 1. Norm-based metrics.

Name of Metric	Equations
Weighted Integrate Factor	$\sqrt{\frac{\sum \max(r_n^2,t_n^2)\left(1-\frac{\max(0,r_n,t_n)}{\max(r_n^2,t_n^2)}\right)^2}{\sum \max(r_n^2,t_n^2)}}$
Zilliacus error	$\frac{\sum \lvert t_n-r_n\rvert}{\sum \lvert r_n\rvert}$
RMS error	$\frac{\sqrt{\sum (t_n-r_n)^2}}{\sqrt{\sum t_n^2}}$
Theil's inequality	$\frac{\sqrt{\sum (t_n-r_n)^2}}{\sqrt{\sum t_n^2}+\sqrt{\sum r_n^2}}$
Whang's inequality	$\frac{\sum \lvert t_n-r_n\rvert}{\sum \lvert t_n\rvert+\sum \lvert r_n\rvert}$
Regression efficient	$\sqrt{1-\frac{(n-1)\sum (t_n-r_n)^2}{n\sum (r_n-\bar{r})^2}}$

performance of the proposed scheme. The conclusions are presented in the last section.

II. A REVIEW OF THE EXISTING COMPARISON SCHEMES

Up to now, various comparison schemes have been proposed and employed by researchers to validate the vehicle safety simulations. In these methods, the stochastic metrics focus on the distribution of the residuals between the signals from test and simulation, see for instance [6]–[8] and the references therein. Although they consider the uncertainties of parameters, the features of original signals are lost. For this reason, only the deterministic metrics will be introduced and discussed in this section.

A. BASIC METRICS

The basic metrics refer to those metrics which involve only one error measure. Compare to the composite metrics, the basic metrics can only reflect the difference on one particular aspects of time histories.

L_1 and L_2 norms of residual signals are the most popular metrics. Generally, they are used to measure the magnitude errors. As a common mathematical tool, the norm can also be used to measure the errors on other aspects, such as time error and frequency error. The shortage of using norms can be listed in twofold: 1) the norms are not normalized and 2) the norms are highly depended on the number of time points. To overcome this shortage, many uniformed metrics are proposed. Some typical ones are listed in Table 1. (Note: r_i means the reference signal, t_i stands for the test and n is the number of sample points.)

Different from the norm methods considering the errors, the coefficient of correlation

$$\rho = \frac{n\sum_{i=1}^{n} t_i r_i - \sum_{i=1}^{n} t_i \sum_{i=1}^{n} r_i}{\sqrt{n\sum_{i=1}^{n} t_i^2 - \left(\sum_{i=1}^{n} t_i\right)^2}\sqrt{n\sum_{i=1}^{n} r_i^2 - \left(\sum_{i=1}^{n} r_i\right)^2}} \quad (1)$$

reflects on how much degrees a signal can be determined by the other one. However, this method is too sensitive to the time error. So the cross-correlation coefficient (also called sliding dot product) is modified from the coefficient of correlation, shown in Eqn. (2), as shown at the bottom of the next page. It is a good measure of time delay (i.e., phase errors) [9], [10] and used in some composite metrics.

Each of these basic metrics can hardly describe the difference effectively, but they provide some tools to develop composite metrics. To achieve better performance, a composite metric may consider the discrepancy on various aspects, including the magnitude, phase or time-of-arrival (TOA), frequency or slope, shape, etc. Different measures will be designed specifically for each kind of features and combined into a comprehensive assessment. According to different features involved, composite metrics can be divided into several groups.

B. MAGNITUDE-PHASE-COMPOSITE (MPC) METRICS

MPC metrics measure the discrepancies on two axes, i.e. the amplitude axis and time axis. Four typical MPC metrics are listed in Table 2.

For the magnitude discrepancy, the first three metrics from Geer share the same measure, while the Russell's measure modifies it to be symmetric. The symmetry keeps the same measure no matter to select which signal as the reference. But this advantage is not significant in model validation as the signal of the real test is commonly chosen as a reference. The measure of phase discrepancy in S&G and Russell is an improvement of that in Geer with a more clear meaning. All of these MPC metrics use the root-sum square of magnitude and phase as the composite result.

Reference [2] compared these metrics mentioned above (except the cross correlation coefficient) with a case study and analyzed the results. As a conclusion, the S&G metric is recommended for the use in roadside safety simulations, such as [11] and [12]. Referencing this suggestion, a computer program for the verification and validation of numerical simulations in roadside safety is developed as RSVVP [13].

C. NORMALIZED INTEGRAL SQUARE ERROR (NISE)

NISE is proposed by Donnelly et al. [14] to quantify the difference between repeated tests. NISE takes the phase, magnitude and shape discrepancies into account with corresponding formulations as follows:

$$M_{NISE} = \rho(n_*) - \frac{2\psi_{rt}(n_*)}{\psi_{rr}+\psi_{tt}} \quad (3)$$

$$P_{NISE} = \frac{2\psi_{rt}(n_*) - 2\psi_{rt}}{\psi_{rr}+\psi_{tt}} \quad (4)$$

$$S_{NISE} = 1 - \rho(n_*) \quad (5)$$

where $\psi_{rr} = \sum r_n^2/N$, $\psi_{tt} = \sum t_n^2/N$, $\psi_{rt} = \sum r_n t_n/N$, n_* is the "steps" to compensate for the error in phase and $\rho(n_*)$ is the cross-correlation in Eqn. (2).

TABLE 2. Typical MPC metrics.

	Magnitude	Phase	Comprehensive
Geers	$M_G = \sqrt{\frac{\sum t_n^2}{\sum r_n^2}} - 1$	$P_G = 1 - \frac{\sum t_n r_n}{\sqrt{\sum t_n^2 \sum r_n^2}}$	$\sqrt{M_G^2 + P_G^2}$
Geers CSA	$M_{GC} = \sqrt{\frac{\sum t_n^2}{\sum r_n^2}} - 1$	$P_{GC} = 1 - \frac{\lvert\sum t_n r_n\rvert}{\sqrt{\sum t_n^2 \sum r_n^2}}$	$sign\left(\sum t_n r_n\right)\sqrt{M_{GC}^2 + P_{GC}^2}$
Sprague & Geers	$M_{SG} = \sqrt{\frac{\sum t_n^2}{\sum r_n^2}} - 1$	$P_{SG} = \frac{1}{\pi}\cos^{-1}\frac{\sum t_n r_n}{\sqrt{\sum t_n^2 \sum r_n^2}}$	$\sqrt{M_{SG}^2 + P_{SG}^2}$
Russell	$M_R = sign\left(m\right)\log_{10}\left(1 + \lvert m\rvert\right), m = \frac{\sum t_n^2 - \sum r_n^2}{\sqrt{\sum t_n^2 \sum r_n^2}}$	$P_R = \frac{1}{\pi}\cos^{-1}\frac{\sum t_n r_n}{\sqrt{\sum t_n^2 \sum r_n^2}}$	$\sqrt{\frac{\pi}{4}\left(M_R^2 + P_R^2\right)}$

The composite metric can be expresses as:

$$C_{NISE} = M_{NISE} + P_{NISE} + S_{NISE} = 1 - \frac{2\psi_{rt}}{\psi_{rr} + \psi_{tt}} \quad (6)$$

Obviously, the measure of shape is cancelled out in C_{NISE}. In addition, the magnitude measure is possible to be negative and then decrease the comprehensive metric.

D. ENHANCED ERROR ASSESSMENT OF RESPONSE TIME HISTORIES (EEARTH)

EEARTH is a comprehensive scheme to evaluate the difference of time histories. The core idea is the EARTH, presented in [1] and [15]. The EARTH metric is the composition of the measures of magnitude, phase and slope. Comparing to other metrics, the EARTH involves the slope as a description of the feature of frequency and therefore improves the assessment significantly. Another valuable idea of EARTH is that to keep the independence of each measure, which means to avoid the influence from other two factors when calculating each measure. Especially, the dynamic time warping (DTW) is employed in the magnitude measure to remove the influence of local time error.

Based on EARTH, the EEARTH scheme proposed by [16] makes the following improvements: 1) translate the original measures into intuitive scores between 0 and 100% and 2) involve an integrated calibration process which incorporates physical-based thresholds and knowledge of subject matter experts (SMEs). The EEARTH is selected into ISO standard ISO/TR16250 and used in many cases, such as [17].

E. SUMMARY AND DISCUSSION

Besides the metrics presented previously, some other metrics, such as Correlation and Analysis (CORA) [18], are also proposed in existing literatures. By studying these metrics, a short summary will be given in this subsection.

1) In general, to make an object and accurate comparison, various features are considered by different metrics. In these features, the magnitude and phase errors are most concerned by researchers. The magnitude error has clear physical meaning and should be measured undoubtedly. However, for vibration signals, the magnitude error will be influenced significantly by the time lag. For this reason, the magnitude measure used in EEARTH has superiority.
2) The measures for phase error are based on the cross-correlation coefficient in most related metrics. Unfortunately, the concept of phase error comes from periodic signals. For non-periodic signals, the cross-correlation coefficient based measures may only qualify the global phase error. That means the local time error is lost in the comparison.
3) Some metrics also try to define the difference of shape. But both the NISE and CORA suffer critical problems. In fact, the shape error can be divided into the errors on magnitude and time axes. In other words, shape error is superfluous if the magnitude and time errors are measured properly.
4) Only EEARTH try to compare the frequency of signals and employ the slope as a substitute. Although not given directly, the frequency, i.e. the oscillation rate of signals is an intuitional information in the comparison.
5) According to the experience of SMEs, some local features are of great value in comparisons, such as the peak values and times [19]. However, they are not included in the existing metrics.

III. AN EEMD AIDED COMPARISON OF TIME HISTORIES

In this section, a novel scheme of time histories comparison is presented in this section. Vehicle crash is a complex process and therefore crash signals contain high frequency

$$\rho\left(n_0\right) = \frac{\left(n-n_0\right)\sum_{i=1}^{n-n_0} t_i r_{i+n_0} - \sum_{i=1}^{n-n_0} t_i \sum_{i=1}^{n-n_0} r_{i+n_0}}{\sqrt{\left(n-n_0\right)\sum_{i=1}^{n-n_0} t_i^2 - \left(\sum_{i=1}^{n-n_0} t_i\right)^2}\sqrt{\left(n-n_0\right)\sum_{i=1}^{n-n_0} r_{i+n_0}^2 - \left(\sum_{i=1}^{n-n_0} r_{i+n_0}\right)^2}} \quad (2)$$

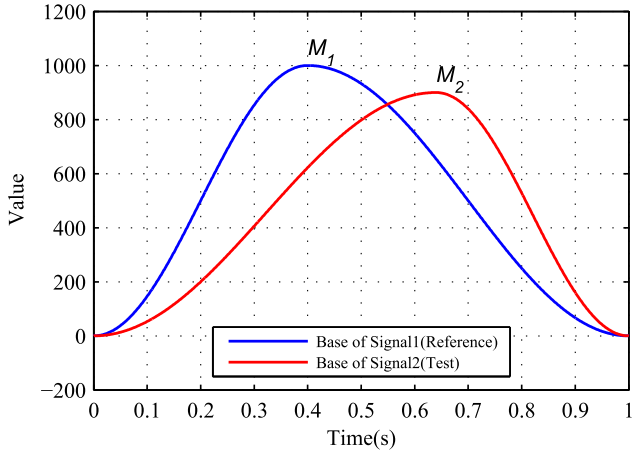

FIGURE 1. Base signals in the example.

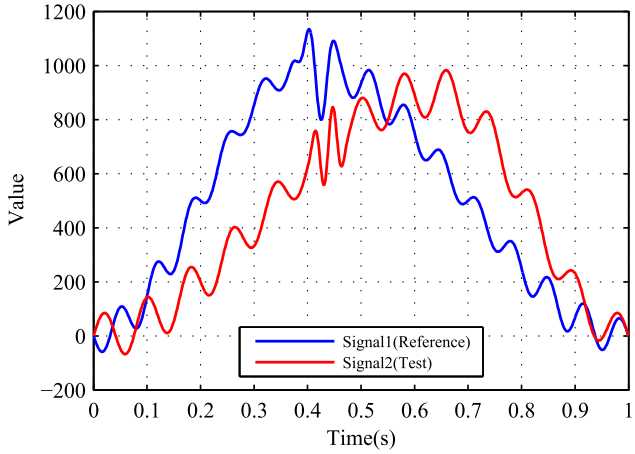

FIGURE 2. Example signals for comparison.

oscillations and uncertainties. According to [20], a crash impulse can be splitted into a "base" and several "shocks," which represent the low and high frequency components respectively. Generally, the "base" reflects the global trend of crash signal and can be decomposed as time and magnitude orthogonally. And the "shocks" may contain the frequency and local features of original signal, which should be analysed and checked to achieve a comprehensive result. In fact, the "shocks" of crash signals have two different catalogues. The first catalogue "shocks" occur in a specified period and keep zero in other time, which can be called as "pulse". While the others are sustained oscillations existing in the whole duration. The basic idea of the proposed scheme is to compare the "base" and "shocks" separately and get more meaningful comparison.

To illustrate the proposed scheme, a pair of signals are used as an example. Each signal consists three components:

$$X = S + P + O \tag{7}$$

where, S, P and O refer to the "base", "pulse" and "oscillation", respectively. In this example, the base pulses are shown as Fig. 1, whose peak points are $M_1 = (0.40s, 1000)$ and $M_2 = (0.64s, 900)$. As shown, the test signal are later and smaller than the reference.

The P and O are given as follows:

$$\begin{cases} P_c = A_1(t) * \sin(40\pi t + \pi) & 0.367 \le t \le 0.467 \\ P_m = A_2(t) * \sin(50\pi t) & 0.400 \le t \le 0.480 \end{cases} \tag{8}$$

and

$$\begin{cases} O_c = A_3(t) * \sin(30\pi t - \pi) \\ O_m = A_4(t) * \sin(25\pi t - \pi) \end{cases} \tag{9}$$

where $A_1(t) = 180\sin^2(10\pi(t - 0.367))$, $A_2(t) = 200\sin^2(12.5\pi(t - 0.367))$, and $A_3(t) = 60 + 12\sin(5\pi t)$ and $A_4(t) = 80 + 10\sin(4\pi t)$. The subscript c refers to the reference signal and m refers to the test signal. The signals for comparison are shown in Fig. 2. Comparing with the reference signal, the test signal has a phase error of 14.54% and a magnitude error of −9.78%, which are calculated by S&G metric.

A. PRE-PROCESSING OF SIGNALS

As many other schemes, the pre-processing of signals is required before comparisons. For a pair of time histories, one of them (generally the signal measured from full car test) is selected as reference signal, and the other one is test signal. Typically, the pre-processing includes:

- Filtering: the influence of noise from measurements should be removed by the filtering of raw data. The digital filters can be designed for different purposes in vehicle safety according to the standard SAE J211.
- Re-sampling: two signals should share the same sampling interval.
- Synchronizing: ensure two crash signals start at the same stage. This step is always operated manually.
- Trimming: For the convenience and accuracy of comparison, the trimming process cuts off the unconcerned period and ensure two signals have the same length.

The Matlab based interactive interface RSVVP provides a friendly tool for pre-processing. More information can reference to [13] and will not be discussed in this paper.

B. ENSEMBLE EMPIRICAL MODE DECOMPOSITION (EEMD)

To extract the trends of crash responses, original signals should be decomposed according to the frequency. The wavelet transformation (WT) has been applied in the model validation [21] and vehicle crash studies [22]. However, the crash responses are nonlinear and non-stationary signals in most cases and the selection of mother wavelet for crash signals is difficult. For this reason, Ensemble Empirical Mode Decomposition (EEMD) is employed in the proposed scheme.

According to Huang and Wu [23], a signal can be decomposed into a set of Intrinsic Mode Functions (IMFs), which represent the natural oscillatory modes embedded in the signal. The instantaneous frequency and amplitude of each time point on IMFs is of physics meaning. The goal of Empirical Mode Decomposition (EMD) is to acquire the IMFs of signal. Different from Fourier Transform and Wavelet Transform, EMD does not suppose any base function and conducts the

decomposition according to the local time scale character of signals. EMD is a self-adaptive time-frequency analysis method for nonlinear and non-stationary signals and therefore suitable for the analysis of crash signals. Given a signal $x(t)$, the procedure of extracting IMFs is called shifting process, shown as Algorithm 1.

Algorithm 1: Shifting Process of EMD

Step 1: Set $p = 1$, $h_p(t) = x(t)$; $q = 0$, $r_q(t) = h_p(t)$.

Step 2: Extract the local maxima and minima of signal $r_q(t)$ and construct the upper and lower envelops of $r_q(t)$ by interpolation method (generally the cubic spline function).

Step 3: Calculate the mean of the upper and lower envelops, recorded as $m_q(t)$. Set $r_{q+1}(t) = r_q(t) - m_q(t)$.

Step 4: Calculate the standard division between $r_q(t)$ an $r_{q+1}(t)$: $SD = \sum \left[r_q(t) - r_{q+1}(t)\right]^2 \Big/ \sum r_q^2(t)$.

Step 5: If $SD \leq threhold$, then stop the shifting process; or else repeat Steps 2∼4 until $SD \leq threhold$. After the shifting process, the residual signal $r_i(t)$ is the IMF_p.

Step 6: Repeat the shifting process (Steps 1∼5) for signal $h_{p+1}(t) = h_p(t) - IMF_p$ to get other IMFs until the IMF_p has only one or no extrema.

EEMD is an improvement of EMD to overcome the mode mixing problem caused by intermittence [24]. In EEMD method, some trial decompositions of noised signals are conducted. The noise here is white noise with finite amplitude. The true IMF component is defined as the mean of an ensemble of trials. Because the noise in each trial is different, the added noise will be filtered by EMD process. With this improvement, EEMD can perform a stable decomposition of original signal. Each IMF from EEMD may fall into a specific frequency interval.

For model validation purposes, only first k IMFs should be treated as ''oscillations'' and the rest IMFs and residual are summated as ''trend''. Then the original signal is written as $X = \sum_{i=1}^{k} IMF_i + T$, where T is the trend signal. k is decided by the criterion that the integration of $IMF_1 \sim IMF_k$ are nearly zero.

In this example, signals are decomposed into a trend and two IMFs. Fig. 3 shows the result of trend extraction. It can be seen that trend signals can represent base pulses perfectly.

After EEMD, the reference and test signals are presented as:

$$\begin{cases} C(t) = \sum_{i=1}^{k} c_i + T_c(t) \\ M(t) = \sum_{i=1}^{k} m_i + T_m(t) \end{cases} \tag{10}$$

Generally, $T_c(t)$ and $T_m(t)$ have same number of peaks and valleys. This condition ensures the DTW process in next subsection have a clear physical interpretation.

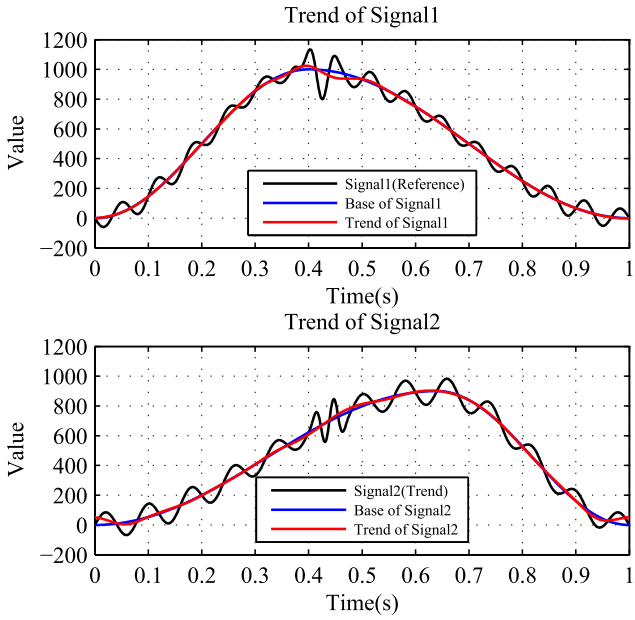

FIGURE 3. Trends of original signals.

C. COMPARE THE TRENDS OF CRASH SIGNALS

The trend signal can be treated as a result of low-pass filtering of original signals and a good representation of base signal. In the comparison of trends, two errors, i.e. Time of Arriving (TOA) and magnitude, are proposed.

The difference of trends can be divided into horizontal (i.e. time) and vertical (i.e. value) directions. To make an orthogonal decomposition of discrepancy, dynamic time warping (DTW) is involved. DTW makes an optimal match between two time histories by expanding or compressing time axes. The cost function of DTW is defined in Eqn. (11) to punish the distance and local shape between two points.

$$d(i,j) = \left((i-j)^2 + (T_c(i) - T_m(j))^2\right) |dT_c(i) - dT_m(j)|^{\alpha} \tag{11}$$

where $dT_c(i) = T_c(i) - T_c(i-1)$, $dT_m(j) = T_m(j) - T_m(j-1)$ and α is an adjustable parameter. Fig. 4 shows correspondence of the trends after DTW. It can be seen that two signals are matched well. Especially, the discrepancy are exactly decomposed along time and value axes.

Comparing with the original signal, the trends are more suitable for DTW process. Fig. 5 shows the warping result of original signals. It can be seen that, local oscillations influence the matching significantly and lead unsuitable warping of signals. For example, the peak point of two signals, i.e. M_1 and M_2 are rematched to N_1 and $N2$ respectively, which are obviously unreasonable.

After the DTW, each time point of test signals has one or several corresponding points in reference signals. Assuming $T_m(i)$ are corresponding to $T_c(p) \sim T_c(q)$ $(p \leq q)$, the error of TOA of $T_m(i)$ is

$$e_t(i) = i - \frac{p+q}{2} \tag{12}$$

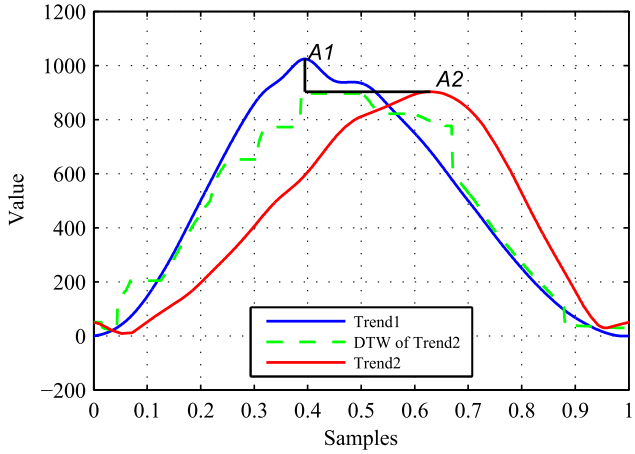

FIGURE 4. Comparison of trend signals.

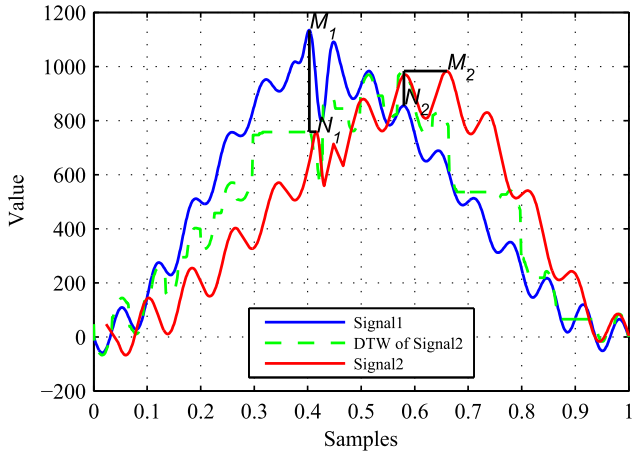

FIGURE 5. DTW of original signals.

And the error of magnitude is

$$e_v(i) = T_m(i) - \frac{\sum_{k=p}^{q} T_c(k)}{q-p+1} \tag{13}$$

Then the discrepancy ratio over the whole time is

$$E_t = \frac{\sum |e_t(i)|}{n^2} \tag{14}$$

$$E_v = \frac{\sum |e_v(i)|}{\sum |T_c(i)|} \tag{15}$$

where n is the length of time history. And the comprehensive error is

$$E = \sqrt{\left(E_t^2 + E_v^2\right)} \tag{16}$$

In the example, $E_t = 10.10\%$, $E_v = 12.28\%$ and $E = 15.90\%$. This result is consistent to the observation and Sprague & Geers metric.

D. COMPARE THE IMFs OF CRASH SIGNALS

The IMFs are series of high frequency oscillations and present the local features of original signals. According to [25], these IMFs are of physical meaning in crash processes. For this reason, comparing the IMFs can achieve more information of vehicle crashworthiness structure. In the proposed scheme,

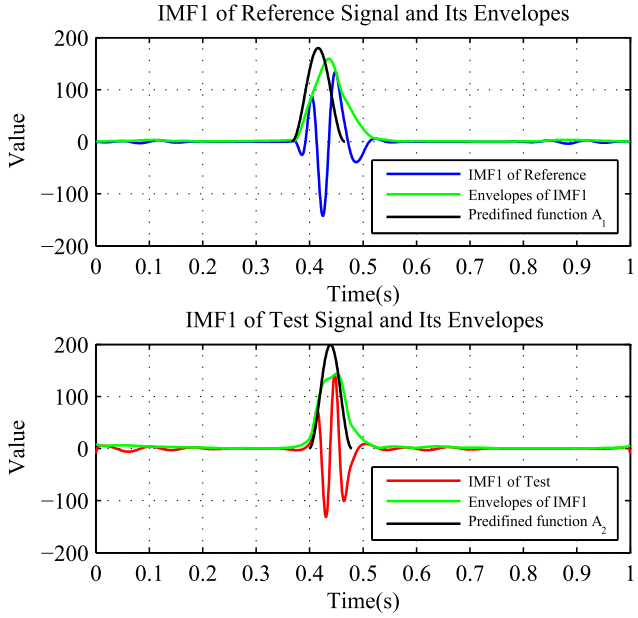

FIGURE 6. Comparison of IMF1.

the error of magnitude and frequency will be compared for validation. However, considering some components in vehicle structure may work in a specified duration, the working period of each IMF should be checked firstly.

According to the property of EEMD, the IMF $x(t)$ is an amplitude modulated-frequency modulated (AM-FM) signal, i.e.,

$$x(t) = A(t)\cos(\varphi(t)) \tag{17}$$

with $A(t) > 0$, $\dot{\varphi}(t) > 0$. To separate the amplitude modulation component $A(t)$ and frequency modulation component $\varphi(t)$, Huang proposed a normalization scheme in [26]. Fig. 6 and Fig. 7 show the IMFs of example signals. As shown, the amplitude functions $A(t)$ are the envelop of IMFs, which are shown by dark line.

The working period is duration $t_a \sim t_b$, when $A(t)$ satisfied $A(t) > A_{th}$. The threshold A_{th} is

$$A_{th} = \theta * \bar{A}(t) \tag{18}$$

where $\bar{A}$ is the average of $A(t)$ and θ is the predefined parameter.

In the example case, the refernece IMF1 has working period $0.381 \sim 0.518s$ and test IMF1 $0.376 \sim 0.522s$. The first pair of IMFs are corresponding to the pulse components. The working period of IMF2s are the whole period, which indicates that IMF2s are corresponding to the oscillations.

The errors of IMFs should be calculated only in corresponding working periods of IMFs. The magnitude error of IMFs is defined as the difference of average amplitude, i.e.,

$$Ea_i = \frac{\bar{A}_{mi}(t) - \bar{A}_{ci}(t)}{\bar{A}_{ci}(t)} \tag{19}$$

where $\bar{A}_{mi}(t)$ and $\bar{A}_{ci}(t)$ are the average amplitude of i-th pair of IMFs.

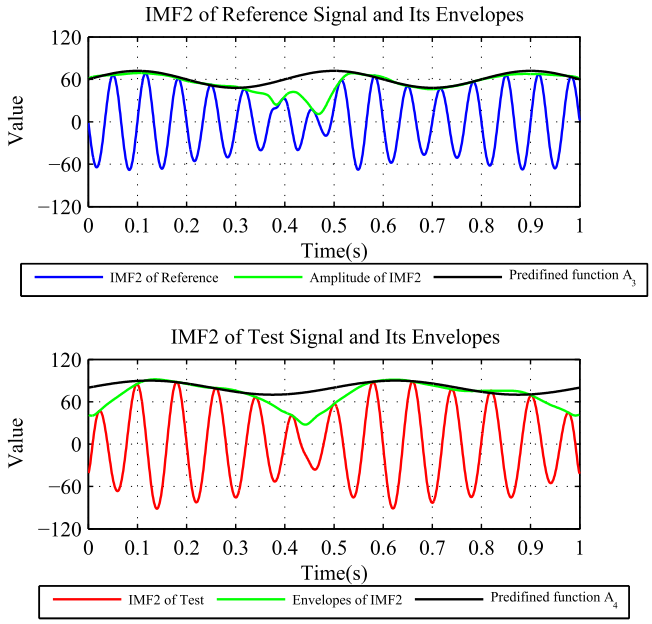

FIGURE 7. Comparison of IMF2.

The instantaneous frequency of $x\,(i)$ can be calculated by

$$f\,(t) = \frac{d\varphi\,(t)}{dt} \tag{20}$$

In the examples, the calculated average frequency of reference IMFs are 17.82Hz and 15.00Hz and of test IMFs are 22.881Hz and 12.95Hz.

The discrepancies of frequency are defineded as

$$Ef_i = \frac{\bar{f}_{mi} - \bar{f}_{ci}}{\bar{f}_{ci}} \tag{21}$$

where $\bar{f}_{mi}\,(t)$ and $\bar{f}_{ci}\,(t)$ are the average frequency of i-th pair of IMFs.

It should be noted that, it is possible that a IMF has no valid working period, which indicates the original signal has no component in the corresponding frequency range. For a pair of IMFs, if both IMFs have no working period, this pair of IMFs can be skipped for comparison. However, if only one IMF has no working period, it may indicate that the component of corresponding frequency is missing in the original signal. In the application of crashworthiness, this may be related to some difference in vehicle structure.

In a short summary, the error metrics of proposed comprehensive comparison scheme are listed in Table 3 with the comparison result of example case. In addition, the working period of IMFs are in Table 4.

IV. CASE STUDY

To demonstrate the proposed scheme, three cases of vehicle crash with different conditions will be employed. According to relative regulations, a new type of vehicle should be checked in full car crash tests before marketing. Generally,

TABLE 3. Comprehensive comparison metrics.

	Metrics	Results
Trend	Time Error	10.49%
	Value Error	12.55%
	Comprehensive	16.35%
IMF1	Magnitude Error	-13.54%
	Frequency Error	28.39%
IMF2	Magnitude Error	28.20%
	Frequency Error	-13.63%

TABLE 4. Working periods of IMFs.

		Reference	Test
IMF1	start	$0.381s$	$0.376s$
	end	$0.518s$	$0.522s$
IMF2	start	$0s$	$0s$
	end	$1s$	$1s$

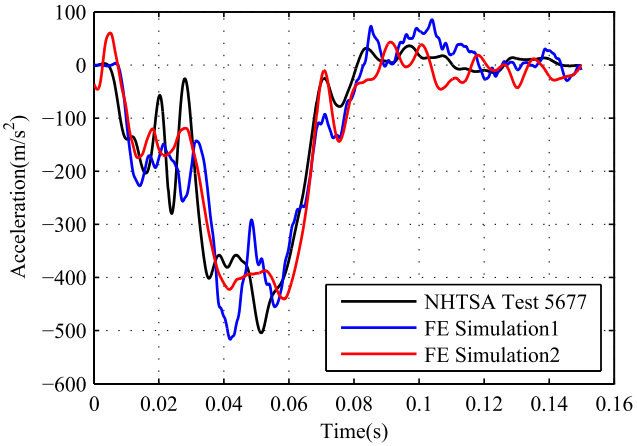

FIGURE 8. Crash responses of left rear seat in 56km/h front crash.

these tests are executed by the New Car Assessment Program (NCAP). To ensure the tests reliable and meaningful, the crashes should be performed in some specified conditions. For example, the FMVSS200 series standards, published by The National Highway Traffic Safety Administration (NHTSA), set the passive safety rules for vehicle crash tests in the US.

In the tests, accelerometers are located on the concerned positions of vehicle body and dummies, such as brake caliper, left rear seat and the head of dummy. These accelerations are recorded as crash responses, which will be used for safety analyses of vehicles. Another source of crash responses are CAE simulations in finite element or multibody software. In this section, the crash responses from CAE software will be compared with those from full car crash, as the common cases of model validation purpose. For simplicity, all signals in this section are sampled by 10kHz and filtered properly.

A. CASE 1

This case is employed to show the basic use of proposed scheme. Fig. 8 shows the crash responses of left rear seat of Toyota Yaris during a 56 km/h front crash. The first signal (reference signal) comes from NHTSA Test 5677 while

another two are from CAE simulations. The FE model of Yaris is published by NCAC and simulated by two different FE softwares. It can be seen that the simulated signals are consistent but have some errors with real crash test. Thus the errors of two simulations are hoped to be similar.

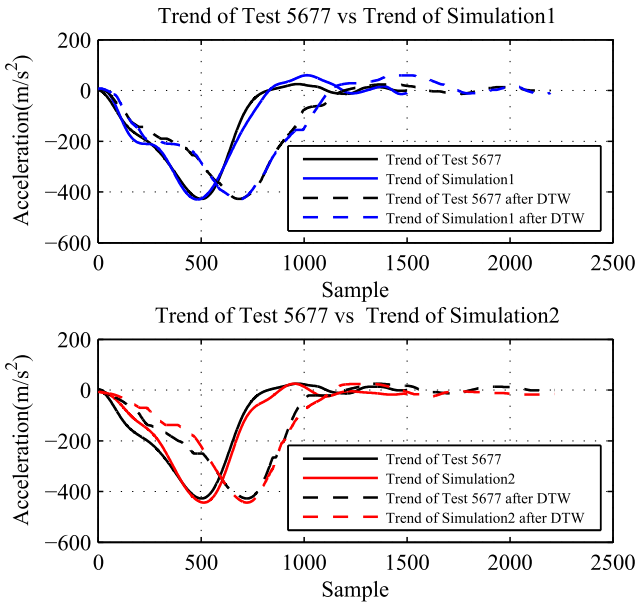

FIGURE 9. Comparison of trends in Case1.

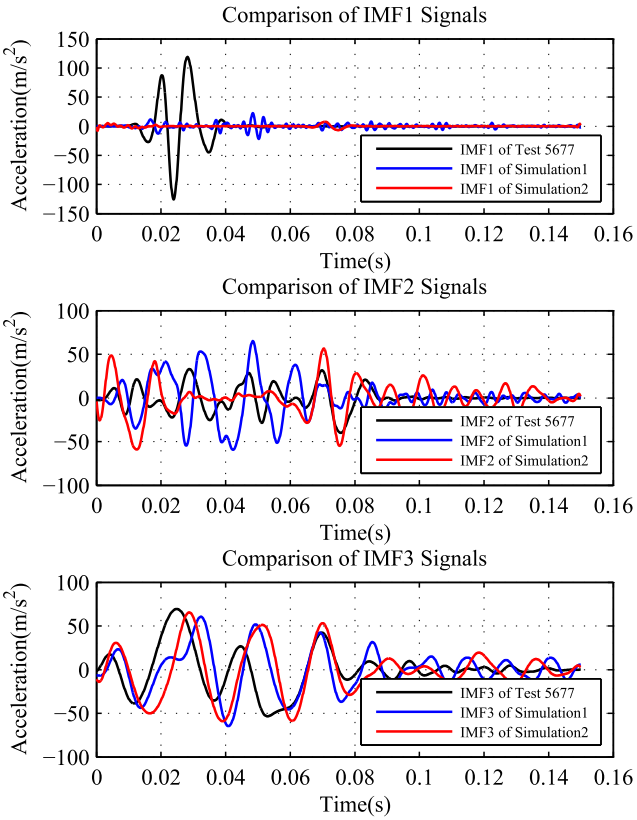

FIGURE 10. Comparison of IMFs in Case1.

Each signal is decomposed as a trend and three IMFs in the EEMD. The trends are shown in Fig. 9. After DTW, the trends are rematched as the dashed lines. As shown, both CAE1 and CAE2 trends match the reference trend very well except in the peak area.

Figure 10 is the comparison of IMFs. It is easy to find a visible discrepancy betweens IMFs, which is corresponding to the error during 0.015∼0.03s of original signals. Other two pairs of IMFs have no significant discrepancy.

Table 5 lists the calculated errors of this case. Based on this table, some notes can be summarised:

1) By checking the errors, both simulation results match the full car crash test very well.
2) Comparing with the result of S&G, the proposed trend comparison achieves smaller error on time axes and bigger magnitude error. This is consistent with the inspection.
3) According to the IMF comparisons, two simulation results have some errors on details. The most important error happens during 0.015∼0.035s of IMF1. This means neither of these two simulations can describe local oscillations well. However, this is not reflected by the given metrics. This is because the time span for comparison is large and the error only exists on a short period. So it is of importance to trim crash responses properly in the pre-processing process.
4) The errors of two simulation results are quite similar. This is reasonable as they are using the same FE model of vehicle. In addition, the common shortage of the two simulations are the lost of oscillations. This error can be seen as the problem of FE model, instead of FE solver.

TABLE 5. Comparison results of Case 1.

		Simulation 1	Simulation 2
Trend	Time Error	2.50%	2.49%
	Value Error	11.70%	16.91%
	Comprehensive	8.46%	12.08%
IMF1	Frequency Error	135.50%	88.52%
IMF2	Frequency Error	7.11%	-4.44%
IMF3	Frequency Error	75.82%	-7.75%
S&G	Phase Error	7.6%	9.7%
	Magnitude Error	-0.6%	1.4%
	Comprehensive	7.6%	9.8%

B. CASE 2

Three signals shown in Fig. 11 are the crash responses of engine top in front crashes, which come from FE simulations. The initial speeds are 56km/h, 48km/h and 40km/h respectively. The proposed scheme is supposed to check the similarity among them.

For the sake of convenience, the crash response of 56km/h crash is set as reference signal. Table 6 presents the results of comparison. Three points are concluded as follows:

1) The main errors exists on the value of magnitude, i.e. the energy of crash. The calculated errors of 40km/h response are bigger than 48km/h response as expectation. An interesting observation is that the error value is related to the square of velocity.

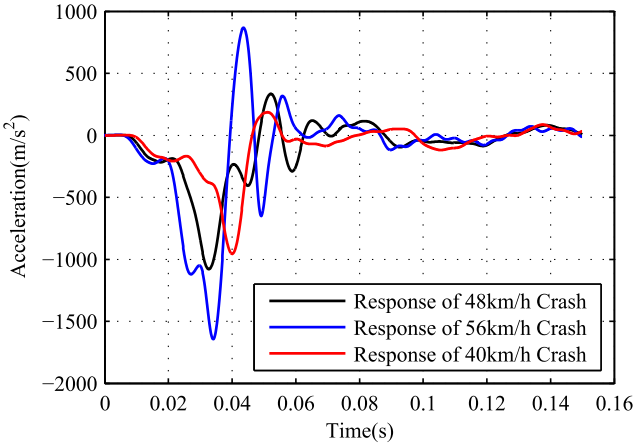

FIGURE 11. Simulated responses of engine top in 56km/h front crashes.

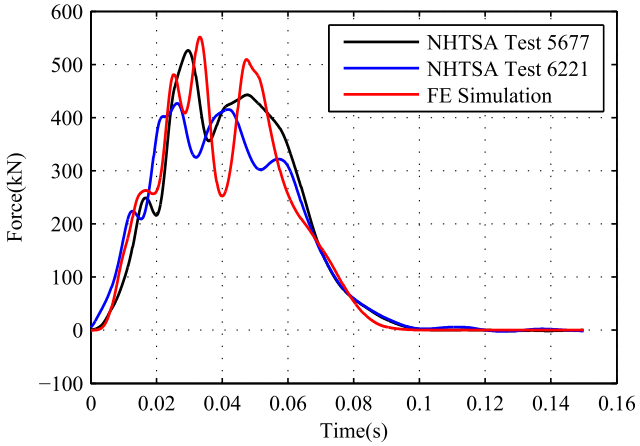

FIGURE 12. External forces in 56km/h front crashes.

TABLE 6. Comparison results of Case 2.

		48km/h Crash	40km/h Crash
Trend	Time Error	2.87%	5.15%
	Value Error	32.83%	28.15%
	Comprehensive	23.30%	20.24%
IMF1	Frequency Error	94.34%	76.49%
IMF2	Frequency Error	39.99%	105.56%
S&G	Phase Error	24.9%	40%
	Magnitude Error	-36.6%	-48.5%
	Comprehensive	44.3%	62.9%

TABLE 7. Comparison results of Case 3.

		Test 6221	FE simulation
Trend	Time Error	6.01%	3.77%
	Value Error	7.34%	1.25%
	Comprehensive	6.70%	2.81%
IMF1	Frequency Error	-40.28%	-34.65%
IMF2	Frequency Error	-39.33%	-22.63%
IMF3	Frequency Error	41.09%	133.66%
S&G	Phase Error	6.8%	6.3%
	Magnitude Error	-9.2%	-1.7%
	Comprehensive	11.4%	6.6%

2) There are very small error of trends on time axes, which is similar to the visual inspection. And comparing to 48km/h crashes, the response of 40km/h crash has a little bigger error of time.

C. CASE 3

Except the acceleration signals, some other time histories can also be compared by the proposed scheme. This case will show an example of comparison of reaction forces from barrier, which is of meaning in vehicle crash analysis. The force signals ares measured in NHTSA Test 5677(reference), NHTSA Test 6221 and an FE simulation. The crash condition is front crash to a rigid wall in 56km/h. NHTSA Test 5677 used Toyota Yaris for test. While Test 6221 used Toyota Yaris 3-Door Liftback, which is a little different on weight and body shape. The FE simulation used the model of Toyota Yaris in NHTSA Test 5677. Figure 12 shows the force signals and Table 7 lists the comparison result.

It can be seen that the results of Test 6221 and FE simulation are quite similar. The trends of them match the reference very well, but the details contain errors. The local error of Test 6221 mainly exists in the frequency component, while that of FE simulation exists on the magnitude aspect. This shows the proposed scheme can distinct small difference again.

V. CONCLUSION

This paper presented an EEMD aided comparison scheme for time histories. Different from other existing methods, each signal for comparison is decomposed into a trend signal and several IMFs. The trend signals and each pair of IMFs are compared separately. The advantages of the proposed scheme are as follows:

1) The trend signal represents the based mode of original signal and is not influenced by high frequency disturbance. The comparison of trend signals will provide a robust result to describe the overall difference between test and reference signal.
2) In the comparison of trends, the DTW process helps to find the corresponding relationship between the nodes of reference and test signals. Based on this, the metric of trend comparison contains two orthogonal discrepancy (i.e. the error of time and value) with clear physical meaning.
3) Each pair of IMFs contains the local information on a specific frequency interval. So the comparison of them is to check the local information. A large error of IMF always refers to the lost of local features, such as peak and local vibration.
4) Another advantage of the proposed scheme is that it involves more features into comparison. This makes it possible to provide a comprehensive result. Especially, the measurement of each feature has clear physical meaning. Therefore the proposed scheme is closed to the comparison of SMEs.
5) In different application areas, some parameters in the proposed method should be adjusted properly. For the

model validation in vehicle safety engineering, the typical values are given in this paper. Another problem to be improved in the future is that some details cannot be reflected by the given metric and need further analysis of IMFs.

REFERENCES

[1] H. Sarin, M. Kokkolaras, G. Hulbert, P. Papalambros, S. Barbat, and R.-J. Yang, "Comparing time histories for validation of simulation models: Error measures and metrics," *J. Dyn. Syst., Meas., Control*, vol. 132, no. 6, p. 061401, 2010.
[2] M. Mongiardini, M. H. Ray, and C. A. Plaxico, "Development of a programme for the quantitative comparison of a pair of curves," *Int. J. Comput. Appl. Technol.*, vol. 46, no. 2, pp. 128–141, 2013.
[3] M. Mongiardini, M. H. Ray, R. Grzebieta, and M. Bambach, "Verification and validation of models used in computer simulations of roadside barrier crashes," in *Proc. Australasian Road Safety Res. Policing Edu. Conf.*, Brisbane, QLD, Australia, 2013, pp. 1–14.
[4] *Instrumentation for Impact Test—Part 1—Electronic Instrumentation*, Standard J211/1_201403, SAE International, 2014.
[5] *Instrumentation for Impact Test—Part 2: Photographic Instrumentation*, Standard J211/2_201406, SAE International, 2014.
[6] Z. Zhan, Y. Fu, R.-J. Yang, and Y. Peng, "Development and application of a reliability-based multivariate model validation method," *Int. J. Vehicle Design*, vol. 60, nos. 3–4, pp. 194–205, 2012.
[7] X. Jiang, R.-J. Yang, S. Barbat, and P. Weerappuli, "Bayesian probabilistic PCA approach for model validation of dynamic systems," SAE International, Tech. Paper 2009-01-1404, Apr. 2009.
[8] Y. Fu, X. Jiang, and R.-J. Yang, "Auto-correlation of an occupant restraint system model using a Bayesian validation metric," SAE International, Tech. Paper 2009-01-1402, 2009.
[9] L. Gu and R. J. Yang, "CAE model validation in vehicle safety design," SAE International, Tech. Paper 2004-01-0455, 2004.
[10] X. Liu, W. Chen, and M. Paas, "Automated occupant model evaluation and correlation," in *Proc. ASME Int. Mech. Eng. Congr. Expo.*, 2005, pp. 353–358.
[11] F. La Torre, L. Domenichini, M. Meocci, A. Nocentini, and S. G. Morano, "Evaluation of the vehicle/safety barrier/sign support interaction by means of FEM simulations," *Int. J. Crashworthiness*, vol. 20, no. 2, pp. 123–133, 2014.
[12] O. Polach and A. Böttcher, "A new approach to define criteria for rail vehicle model validation," *Vehicle Syst. Dyn.*, vol. 52, no. sup1, pp. 125–141, 2014.
[13] M. H. Ray, M. Mongiardini, and C. Plaxico, "Quantitative methods for assessing similarity between computational results and full-scale crash tests," in *Proc. 91th Annu. Meeting Transp. Res. Board*, Washington, DC, USA, 2012, pp. 1–21.
[14] B. R. Donnelly, R. M. Morgan, and R. H. Eppinger, "Durability, repeatability and reproducibility of the NHTSA side impact dummy," SAE International, Tech. Paper 831624, 1983.
[15] H. Sarin, M. Kokkolaras, G. Hulbert, P. Papalambros, S. Barbat, and R.-J. Yang, "A comprehensive metric for comparing time histories in validation of simulation models with emphasis on vehicle safety applications," in *Proc. ASME Int. Design Eng. Tech. Conf. Comput. Inf. Eng. Conf.*, 2008, pp. 1275–1286.
[16] Z. Zhan, Y. Fu, and R.-J. Yang, "Enhanced error assessment of response time histories (EEARTH) metric and calibration process," SAE International, Tech. Paper 2011-01-0245, 2011.
[17] J. B. Putnam, C. D. Untaroiu, J. Littell, and M. Annett, "Finite element model of the THOR-NT dummy under vertical impact loading for aerospace injury prediction: Model evaluation and sensitivity analysis," *J. Amer. Helicopter Soc.*, vol. 60, no. 2, pp. 1–10, 2015.
[18] C. Gehre, H. Gades, and P. Wernicke, "Objective rating of signals using test and simulation responses," in *Proc. 21st Int. Tech. Conf. Enhanced Safety Vehicles*, Stuttgart, Germany, 2009, pp. 1–8.
[19] L. E. Schwer, "Validation metrics for response histories: Perspectives and case studies," *Eng. Comput.*, vol. 23, no. 4, pp. 295–309, Dec. 2007.
[20] C. C. Chou, J. Le, P. Chen, and D. Bauch, "Development of CAE simulated crash pulses for airbag sensor algorithm/calibration in frontal impacts," in *Proc. 17th Int. Tech. Conf. Enhanced Safety Vehicles*, Amsterdam, The Netherlands, 2001, pp. 1–12.
[21] J. R. McCusker, K. Danai, and D. O. Kazmer, "Validation of dynamic models in the time-scale domain," *J. Dyn. Syst., Meas., Control*, vol. 132, no. 6, p. 061402, 2010.
[22] H. R. Karimi and K. G. Robbersmyr, "Signal analysis and performance evaluation of a vehicle crash test with a fixed safety barrier based on Haar wavelets," *Int. J. Wavelets, Multiresolution Inf. Process.*, vol. 9, no. 1, pp. 131–149, Jan. 2011.
[23] N. E. Huang and Z. Wu, "A review on Hilbert–Huang transform: Method and its applications to geophysical studies," *Rev. Geophys.*, vol. 46, no. 2, 2008.
[24] Z. Wu and N. E. Huang, "Ensemble empirical mode decomposition: A noise-assisted data analysis method," *Adv. Adapt. Data Anal.*, vol. 1, no. 1, pp. 1–41, 2008.
[25] Z. Wei, H. R. Karimi, and K. G. Robbersmyr, "Analysis of the relationship between energy absorbing components and vehicle crash response," SAE International, Tech. Paper 2016-01-1541, 2016.
[26] N. E. Huang, Z. Wu, S. R. Long, K. C. Arnold, X. Chen, and K. Blank, "On instantaneous frequency," *Adv. Adapt. Data Anal.*, vol. 1, no. 2, pp. 177–229, 2009.

ZUOLONG WEI (M'14) received the B.S. and M.S. degrees in control science and engineering from the Harbin Institute of Technology, Harbin, China, in 2010 and 2012, respectively. He is currently pursuing the Ph.D. degree in mechatronics at the University of Agder, Grimstad, Norway. His research interests include control theory and application, system modeling, signal processing and CAE simulation, especially in the vehicle safety area.

KJELL GUNNAR ROBBERSMYR (SM'15) received the M.Sc. and Ph.D. degrees in mechanical engineering from Norwegian University of Science and Technology, Norway, in 1985 and 1992, respectively.

From 1997 to 2005, he was the Leader of a scientific group working in the area of full-scale crash testing, including, performance evaluation of safety barriers. He is currently a Professor of Machine Design with the University of Agder, Grimstad, Norway. His main research interests include machine design (component and system design, and product development) and vehicle crash simulations (finite-element analysis).

HAMID REZA KARIMI (M'06–SM'09) was born in 1976. He received the B.Sc. degree (Hons.) in power systems from Sharif University of Technology, Tehran, Iran, in 1998, and the M.Sc. and Ph.D. degrees (Hons.) in control systems engineering from the University of Tehran, Tehran, in 2001 and 2005, respectively.

He is currently a Professor of Applied Mechanics with the Department of Mechanical Engineering, Politecnico di Milano, Milan, Italy. His research interests include control systems and mechatronics.

Prof. Karimi is the Editor-in-Chief of the *Journal of DESIGNS* and an Editorial Board Member for some international journals, such as the IEEE TRANSACTIONS ON INDUSTRIAL ELECTRONICS, the IEEE TRANSACTIONS ON CIRCUIT AND SYSTEMS I: REGULAR PAPERS, the IEEE/ASME TRANSACTIONS ON MECHATRONICS, *Information Sciences*, the IEEE ACCESS, *IFAC-Mechatronics, Neurocomputing*, the *Asian Journal of Control*, the *Journal of The Franklin Institute*, the *International Journal of Control, Automation, and Systems*, the *International Journal of Fuzzy Systems*, the *International Journal of e-Navigation and Maritime Economy*, and the *Journal of Systems and Control Engineering*. He is also a member of the IEEE Technical Committee on Systems with Uncertainty, the Committee on Industrial Cyber-Physical Systems, the IFAC Technical Committee on Mechatronic Systems, the Committee on Robust Control, and the Committee on Automotive Control. He received the 2016 Web of Science Highly Cited Researcher in Engineering.